Electronic Supplementary Material (ESI) for Green Chemistry.
This journal is © The Royal Society of Chemistry 2023

Electronic Supplementary Information for

Visible-light-driven anaerobic oxidative upgrading of biomass-derived HMF for co-production of DFF and H_2 over 1D $Cd_{0.7}Zn_{0.3}S/NiSe_2$ Schottky junction

Tao Shan, Luteng Luo, Taoran Chen, Lixun Deng, Mengqing Li, Xuhui Yang, Lijuan Shen, Min-Quan Yang*

College of Environmental and Resource Sciences, College of Carbon Neutral Modern Industry, Fujian Key Laboratory of Pollution Control & Resource Reuse, Fujian Normal University, Fuzhou 350007, P.R. China

*Corresponding Author E-mail: yangmq@fjnu.edu.cn

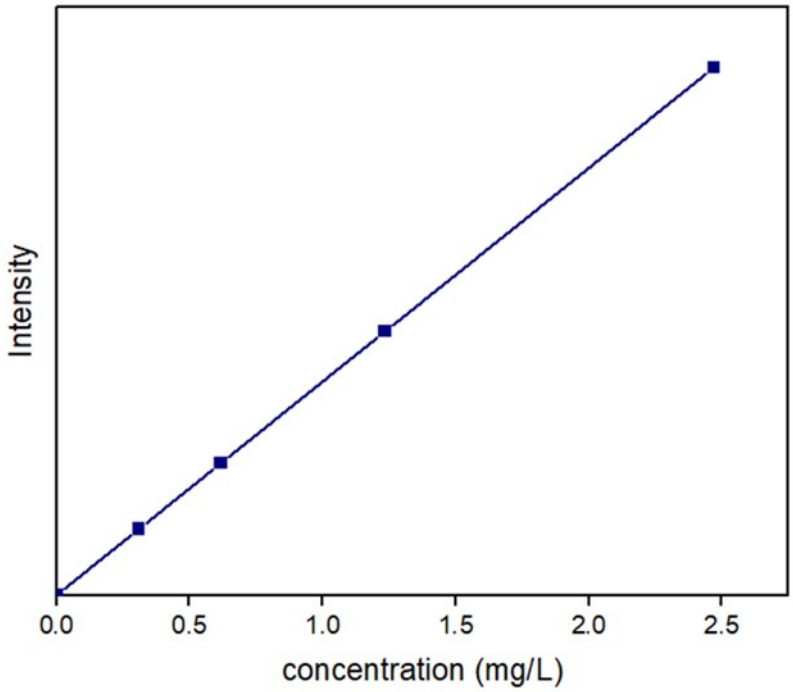

Figure S1. Standard curve of the ICP-OES for Ni^{2+}.

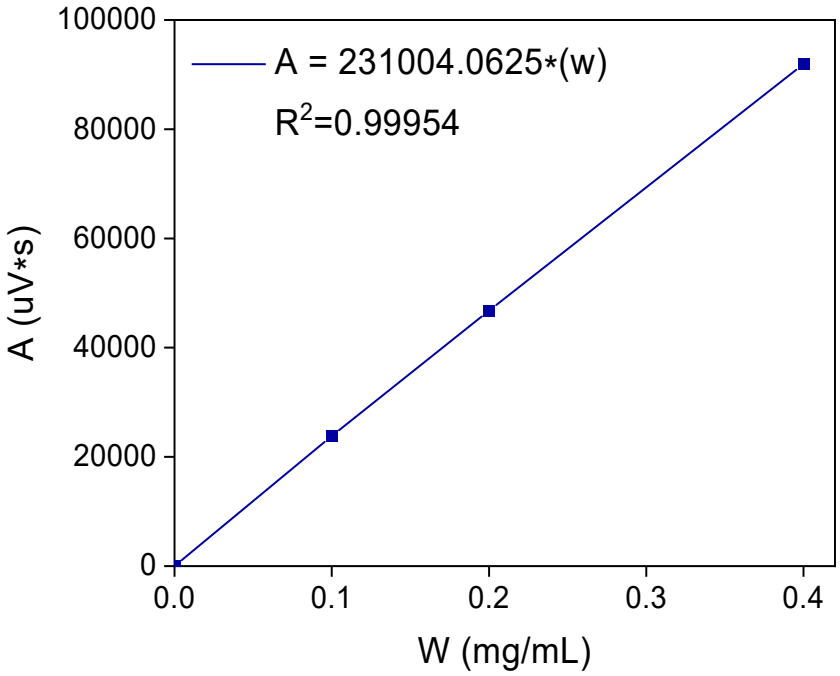

Figure S2. Standard curve of the GC 9790plus for H_2.

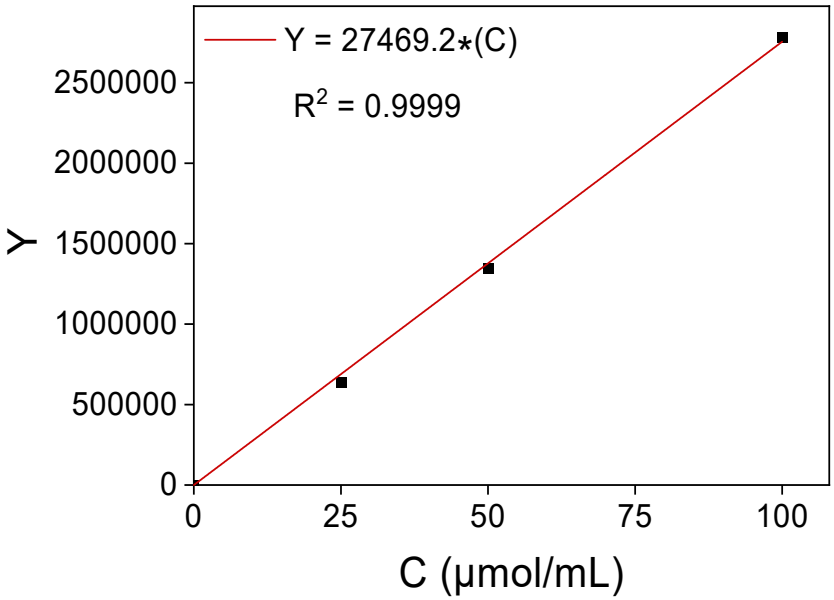

Figure S3. Standard curve of the GC-2030 for DFF.

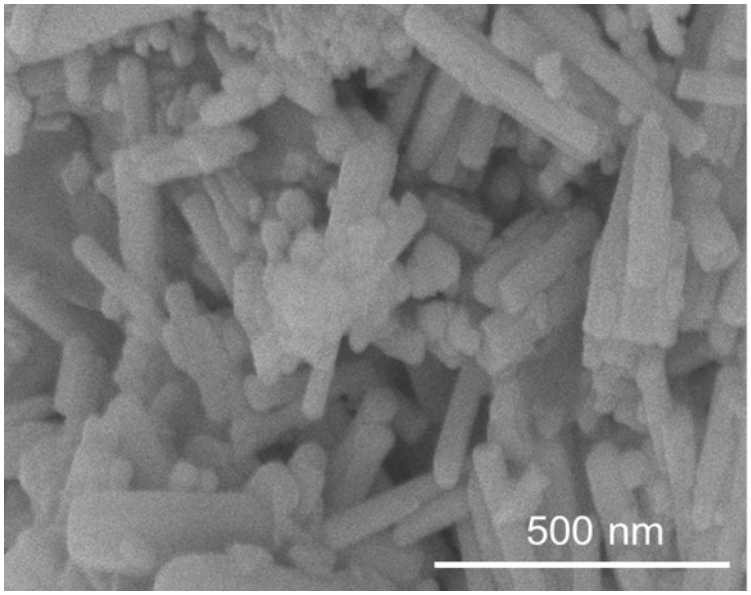

Figure S4. SEM image of CdS.

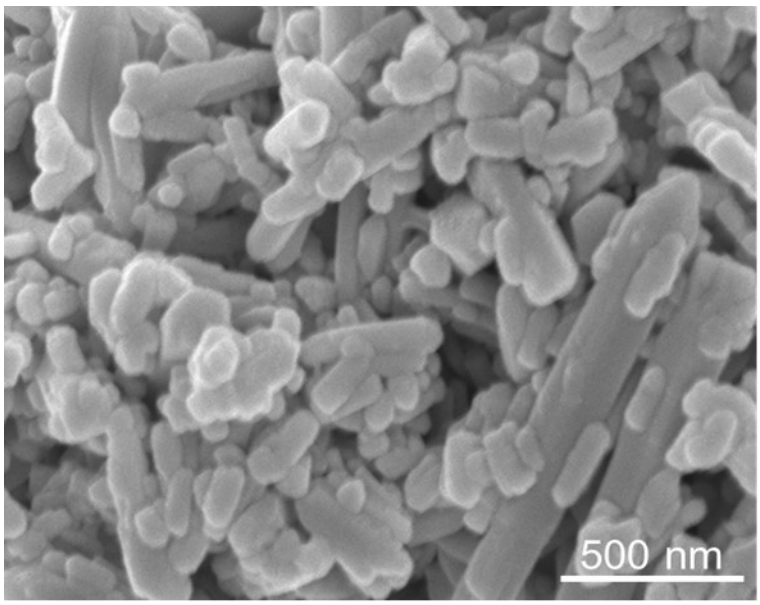

Figure S5. SEM image of $CdS/NiSe_2$ 4%.

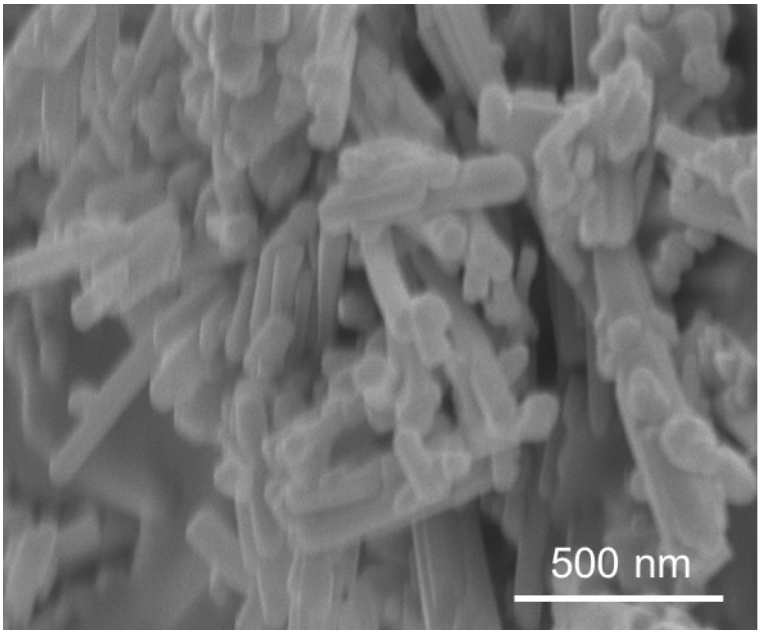

Figure S6. SEM image of $Cd_{0.9}Zn_{0.1}S$.

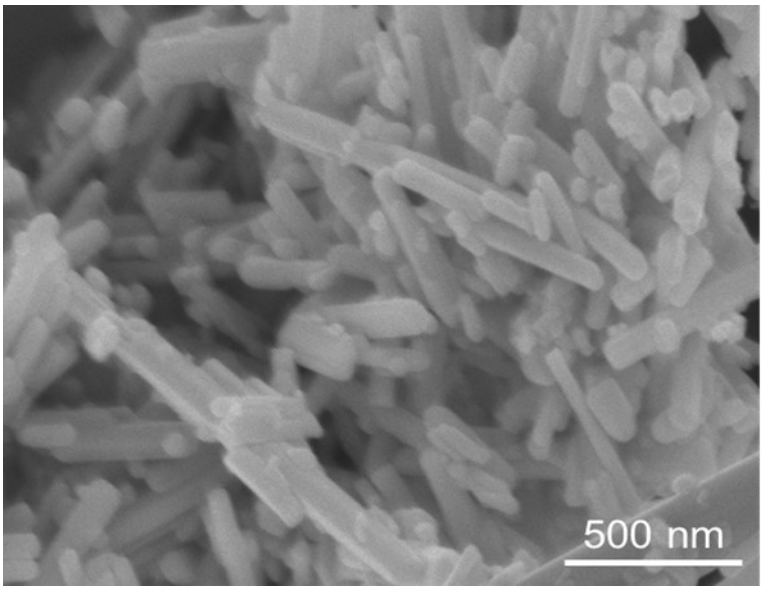

Figure S7. SEM image of $Cd_{0.9}Zn_{0.1}S/NiSe_2$ 4%.

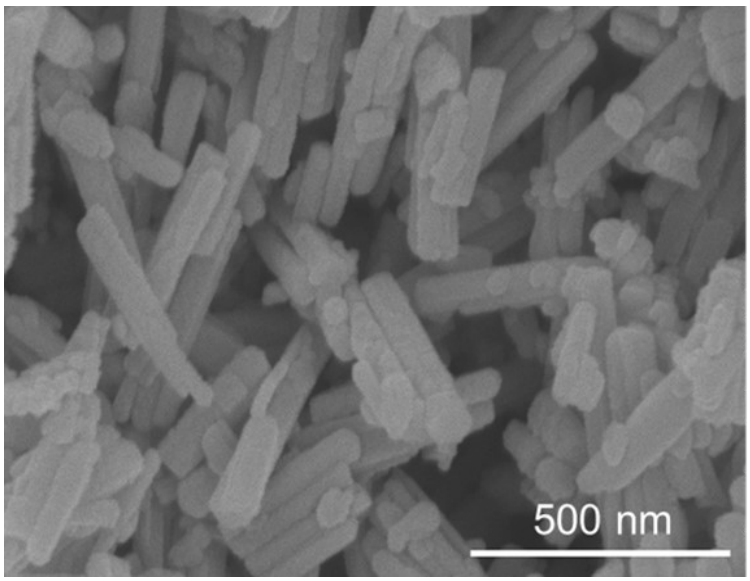

Figure S8. SEM image of $Cd_{0.8}Zn_{0.2}S$.

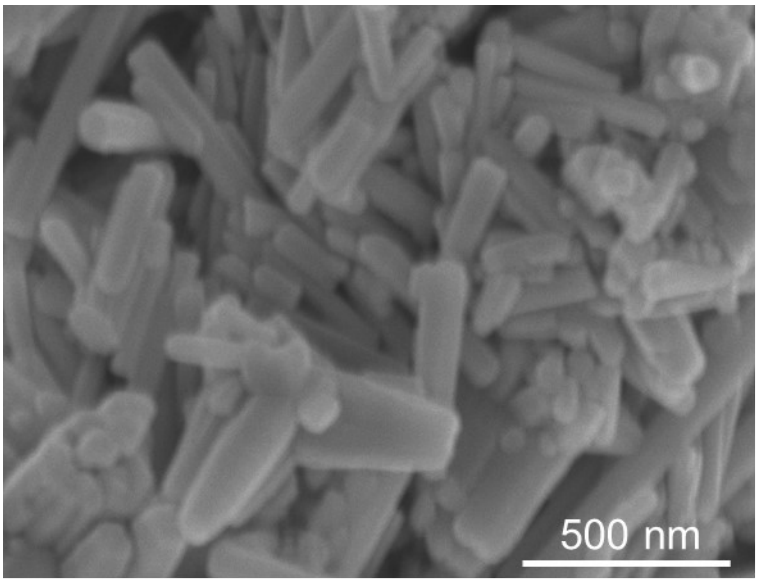

Figure S9. SEM image of $Cd_{0.8}Zn_{0.2}S/NiSe_2$ 4%.

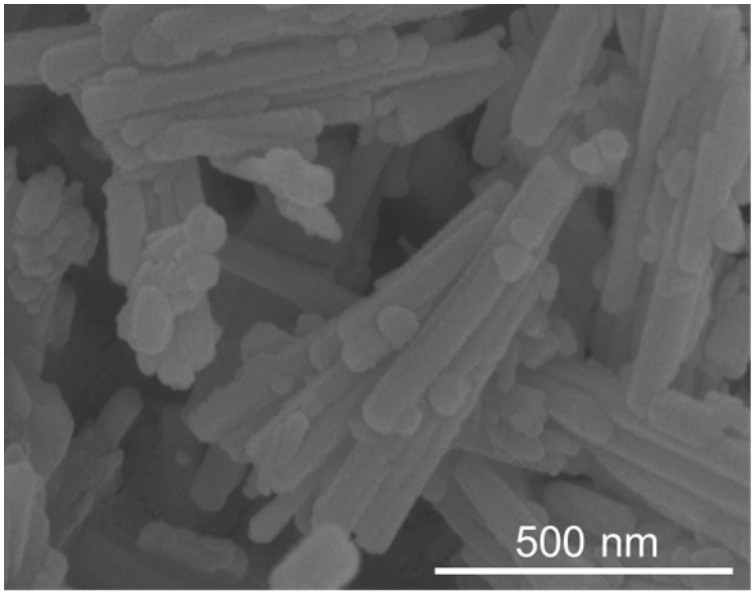

Figure S10. SEM image of $Cd_{0.6}Zn_{0.4}S$.

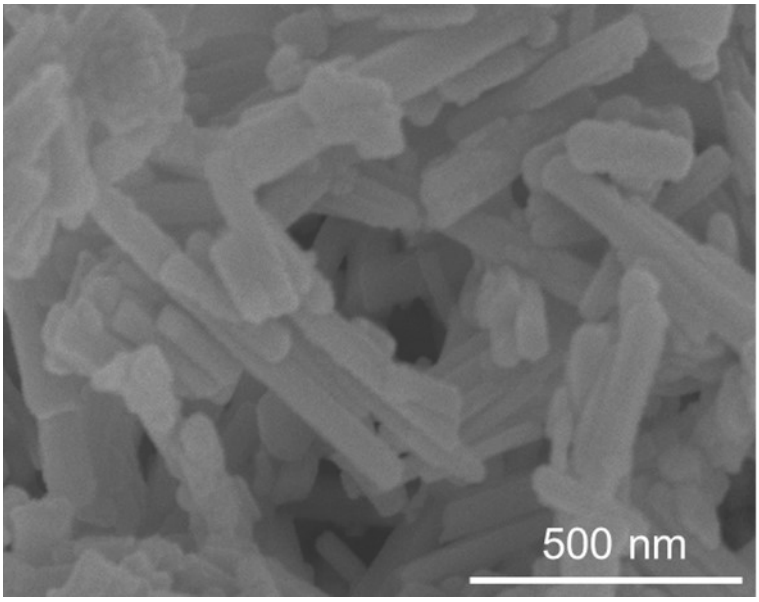

Figure S11. SEM image of $Cd_{0.6}Zn_{0.4}S/NiSe_2$ 4%.

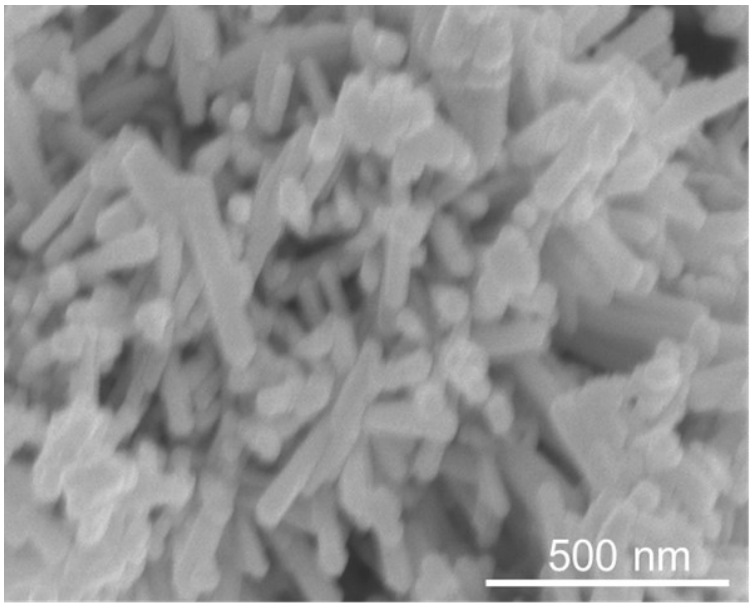

Figure S12. SEM image of $Cd_{0.5}Zn_{0.5}S$.

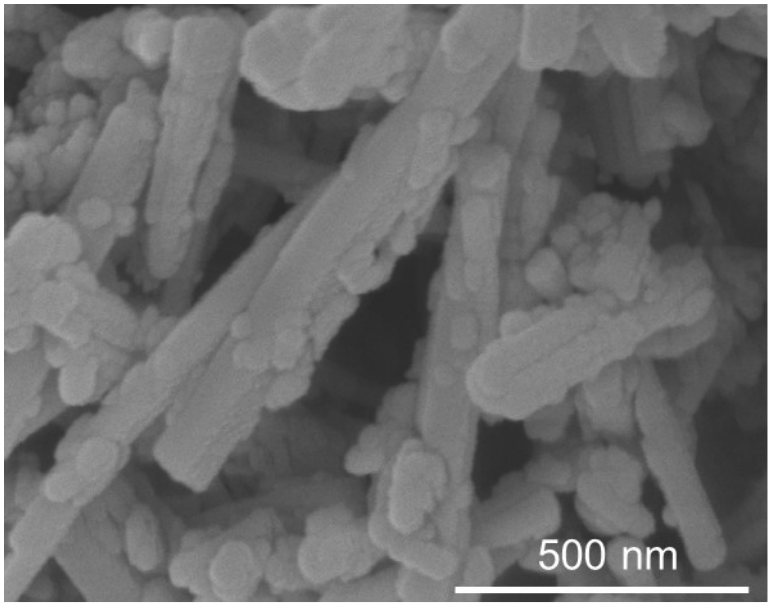

Figure S13. SEM image of $Cd_{0.5}Zn_{0.5}S/NiSe_2$ 4%.

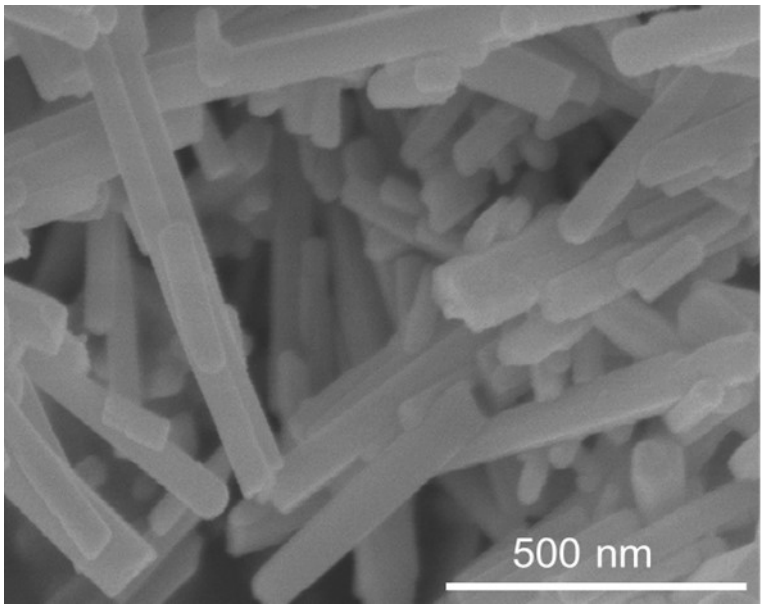

Figure S14. SEM image of $Cd_{0.7}Zn_{0.3}S/NiSe_2$ 2.5%.

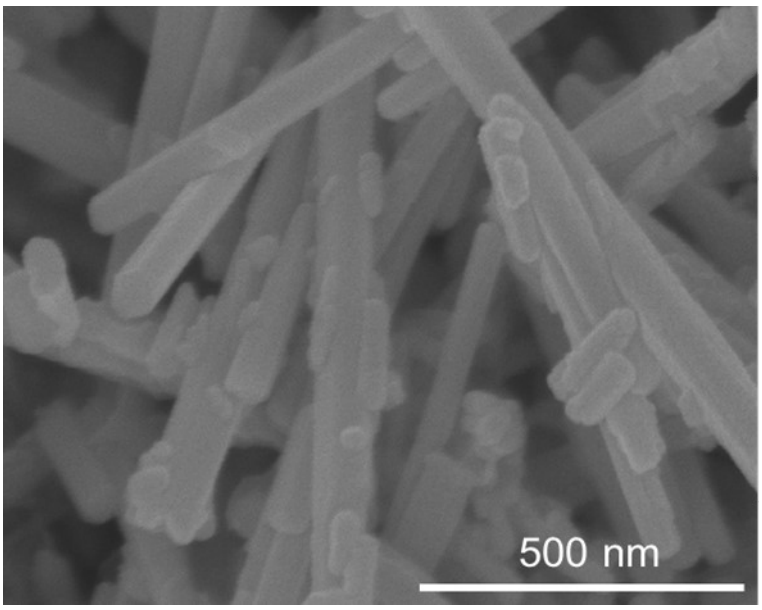

Figure S15. SEM image of $Cd_{0.7}Zn_{0.3}S/NiSe_2$ 3.5%.

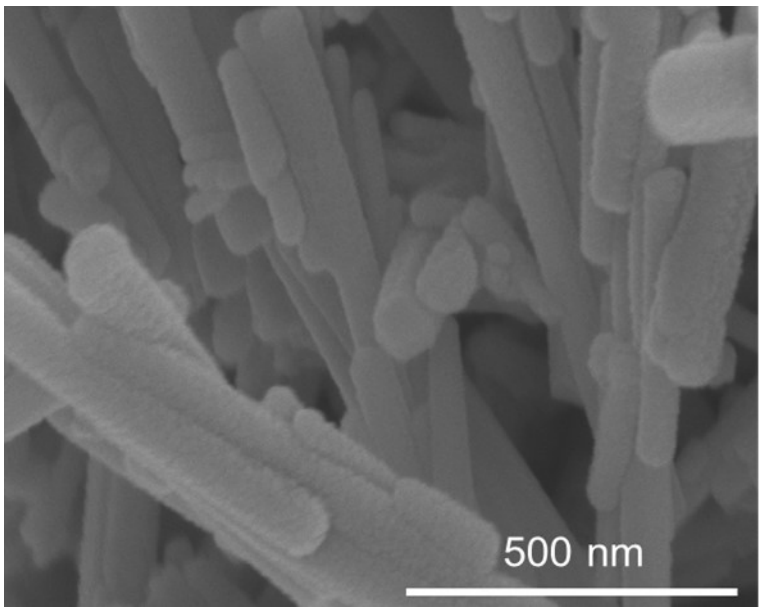

Figure S16. SEM image of $Cd_{0.7}Zn_{0.3}S/NiSe_2$ 4.6%.

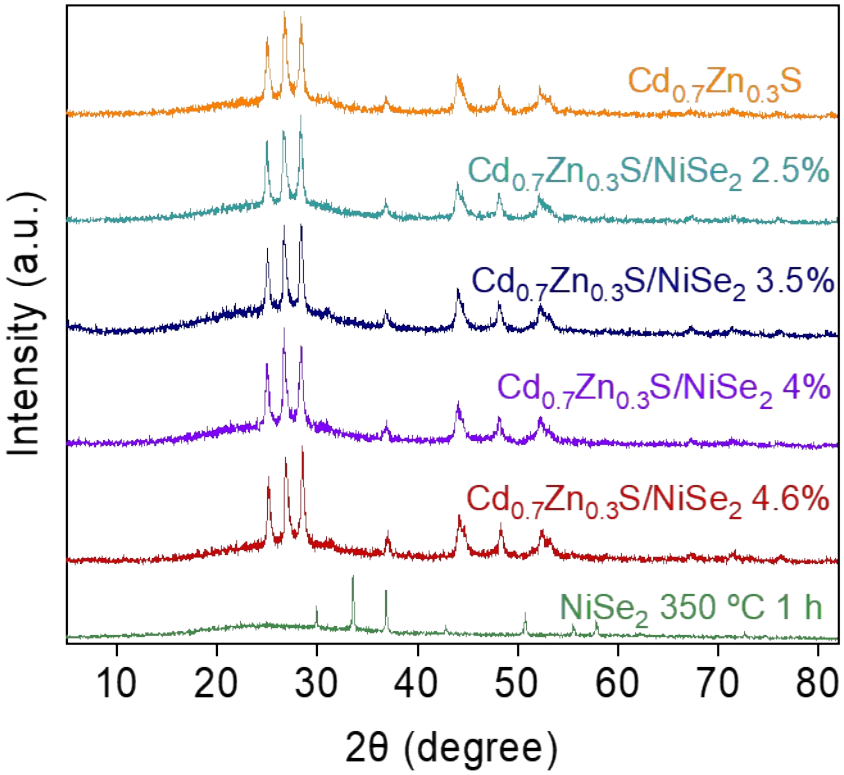

Figure S17. XRD patterns of $Cd_{0.7}Zn_{0.3}S/NiSe_2$ x% composites.

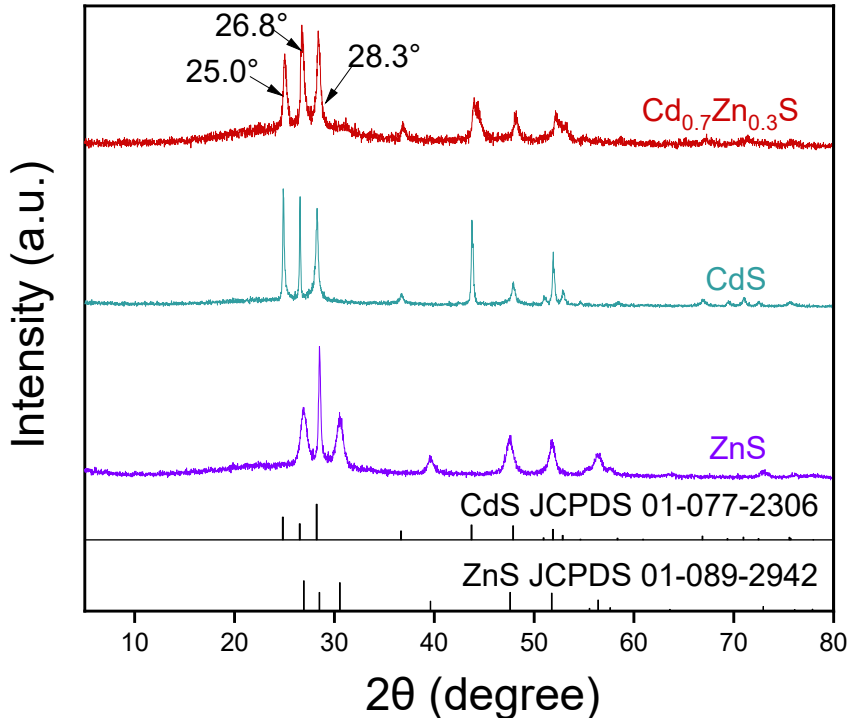

Figure S18. XRD patterns of $Cd_{0.7}Zn_{0.3}S$, CdS, and ZnS.

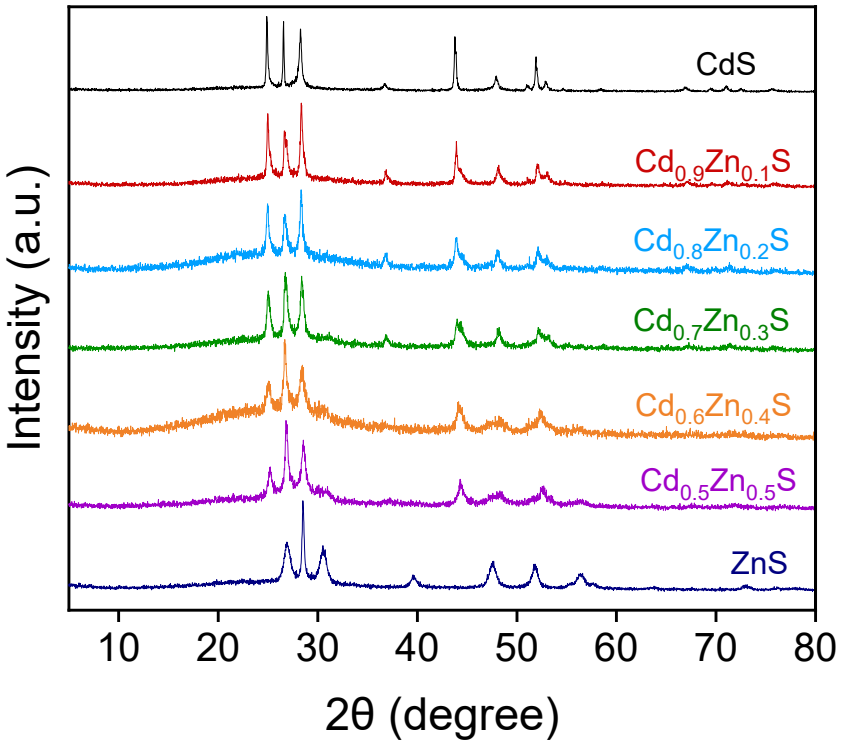

Figure S19. XRD patterns of $Cd_{1-x}Zn_xS$ with different Cd and Zn proportions.

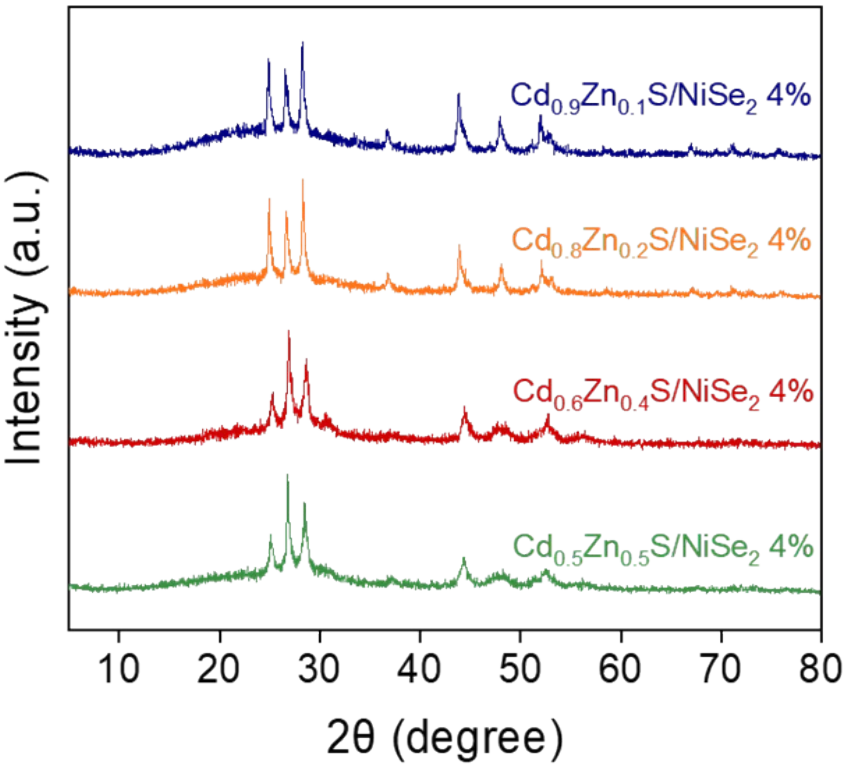

Figure S20. XRD patterns of $Cd_{1-x}Zn_xS/NiSe_2$ 4% with different Cd and Zn proportions.

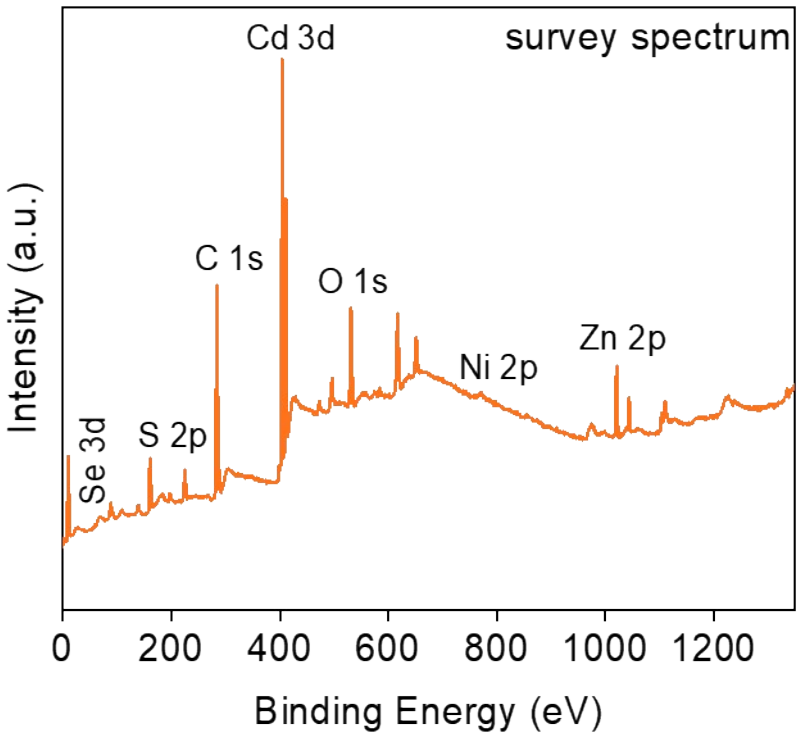

Fig. S21. XPS survey spectrum of $Cd_{0.7}Zn_{0.3}S/NiSe_2$ 4% composite.

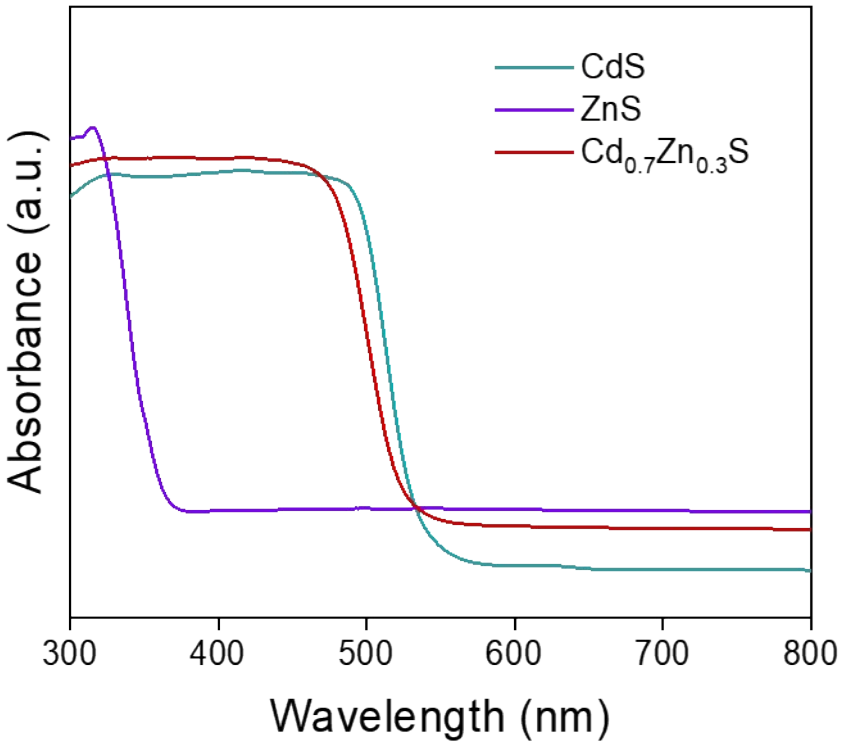

Figure S22. DRS spectra of CdS, ZnS, and $Cd_{0.7}Zn_{0.3}S$ samples.

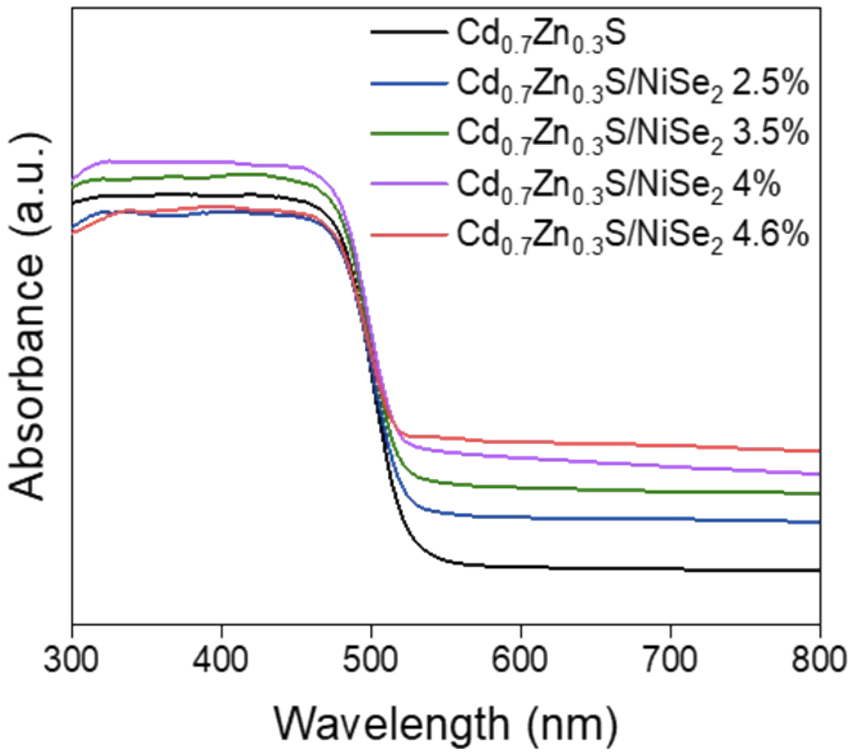

Figure S23. DRS spectra of $Cd_{0.7}Zn_{0.3}S/NiSe_2$ x% samples (x = 0, 2.5, 3.5, 4, 4.6)

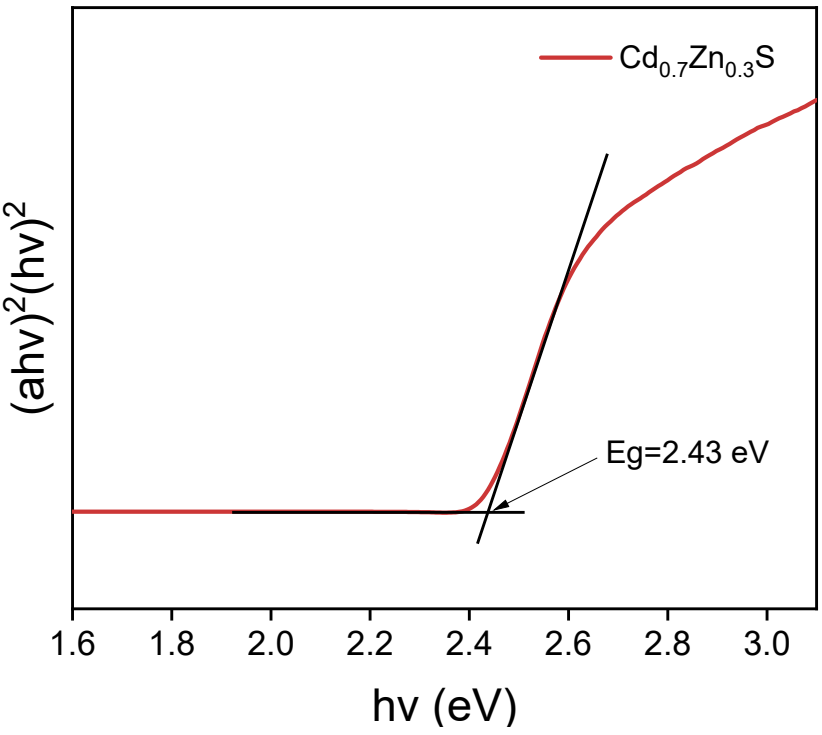

Figure S24. Tauc plot for measuring the bandgap of $Cd_{0.7}Zn_{0.3}S$.

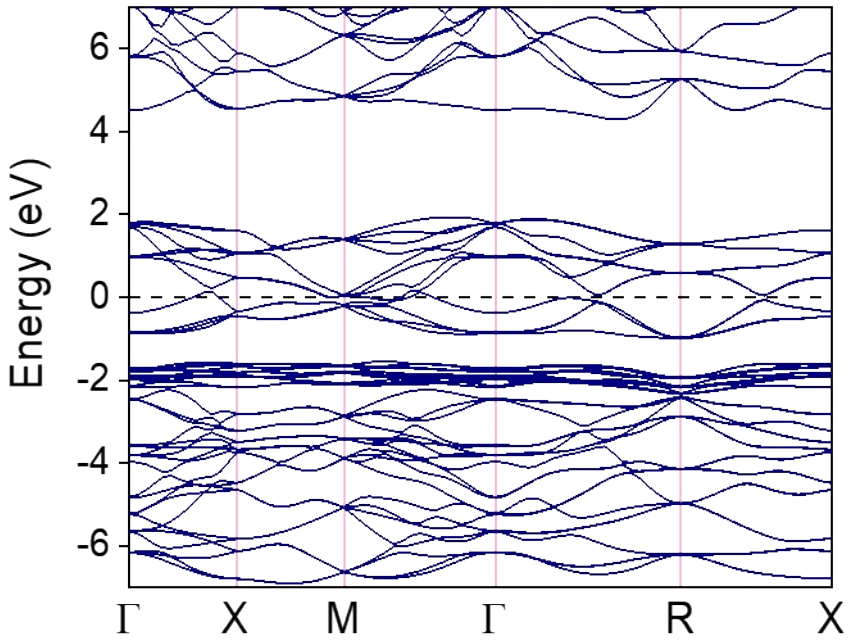

Figure S25. The band structure of bulk $NiSe_2$.

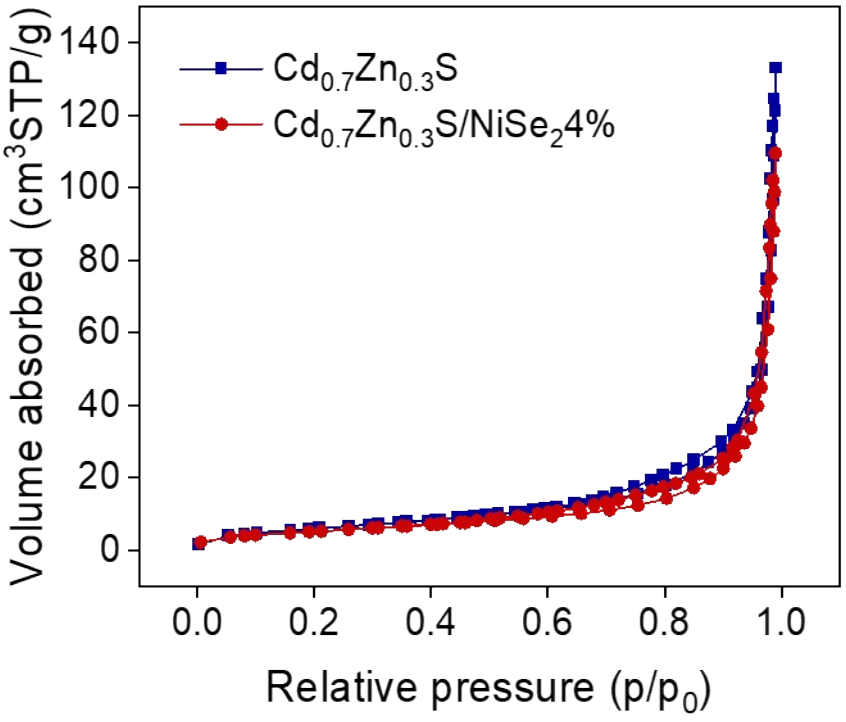

Figure S26. Nitrogen adsorption-desorption isotherms of $Cd_{0.7}Zn_{0.3}S$ and $Cd_{0.7}Zn_{0.3}S/NiSe_2$ 4%.

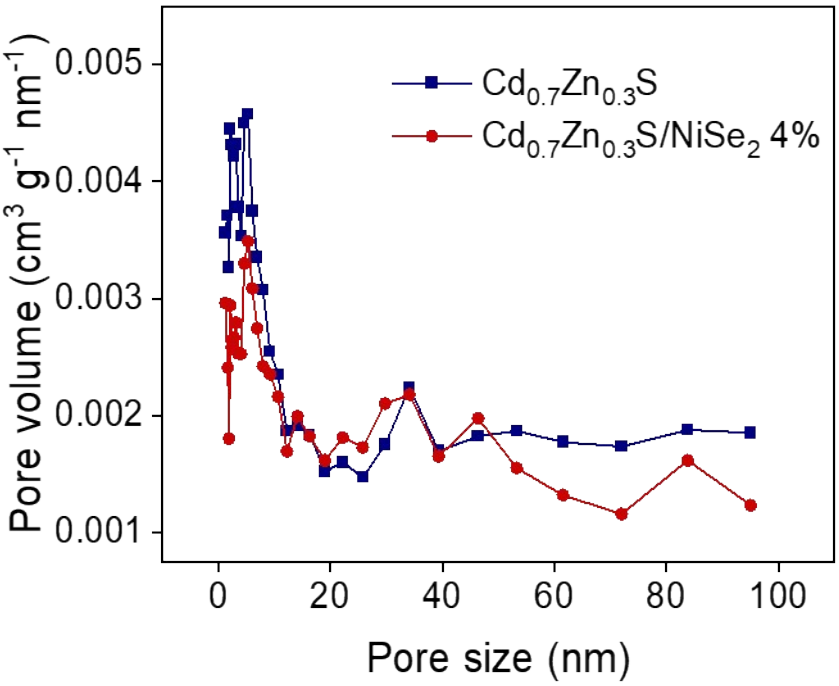

Figure S27. Pore size distribution of $Cd_{0.7}Zn_{0.3}S$ and $Cd_{0.7}Zn_{0.3}S/NiSe_2$ 4%.

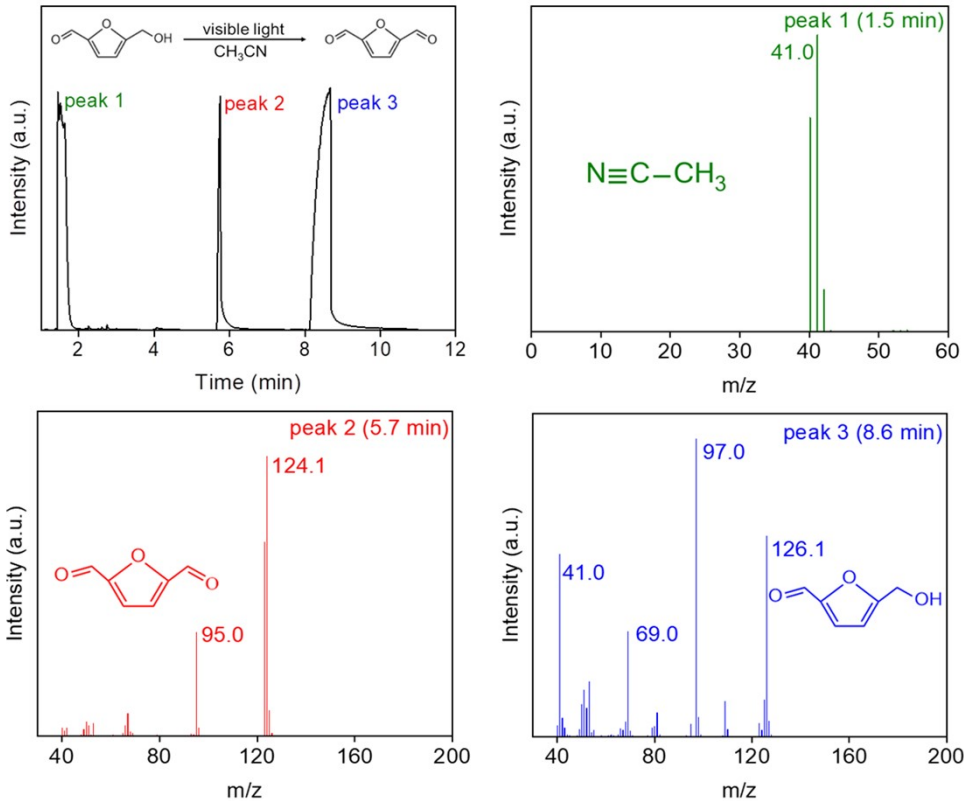

Figure S28. GC-MS spectra of the reaction solution analyzed after photocatalytic experiment. Conditions: 100 μmol HMF, 10 mg $Cd_{0.7}Zn_{0.3}S/NiSe_2$ 4%, 3 mL CH_3CN, 780 nm ≥ λ ≥ 400 nm.

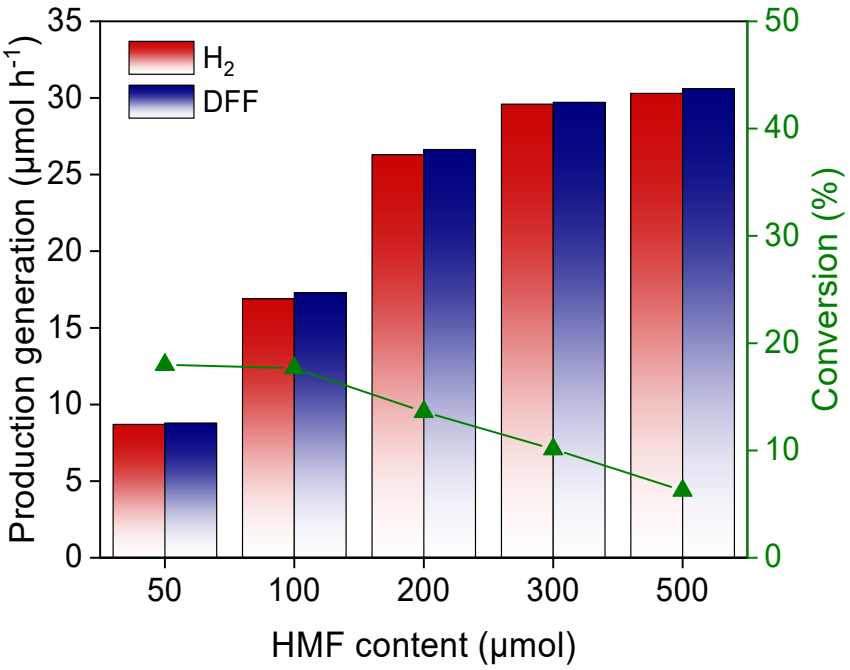

Figure S29. The photoactivity tests of selective HMF oxidation into DFF integrated with H_2 evolution under different concentrations.

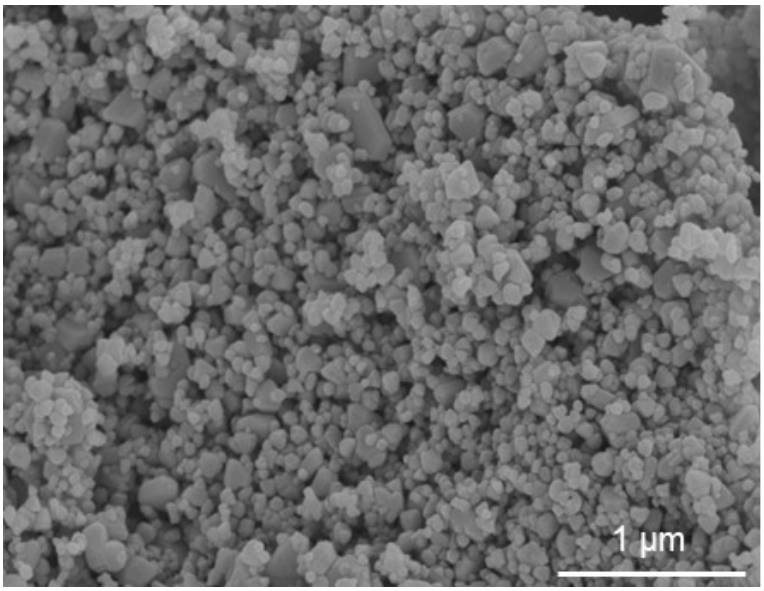

Figure S30. SEM image of $Cd_xZn_{1-x}S$ NPs

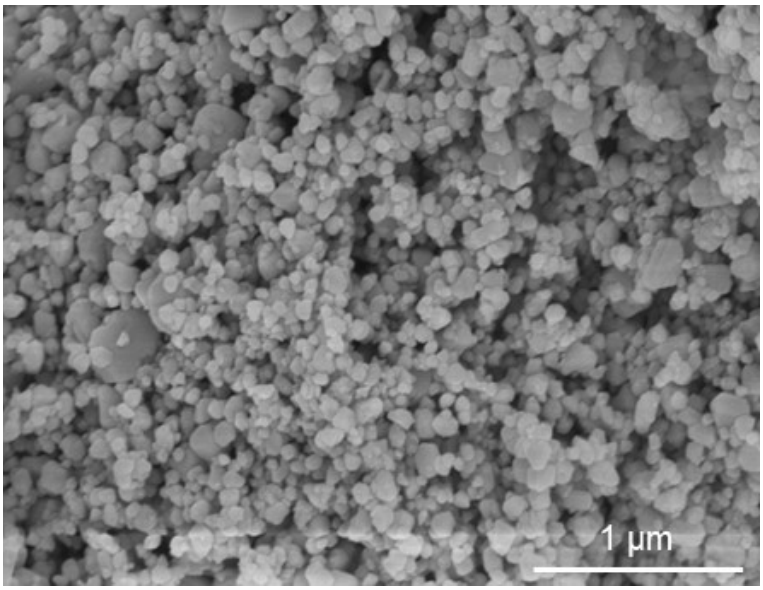

Figure S31. SEM image of $Cd_xZn_{1-x}S$ NPs/$NiSe_2$ 4% composite.

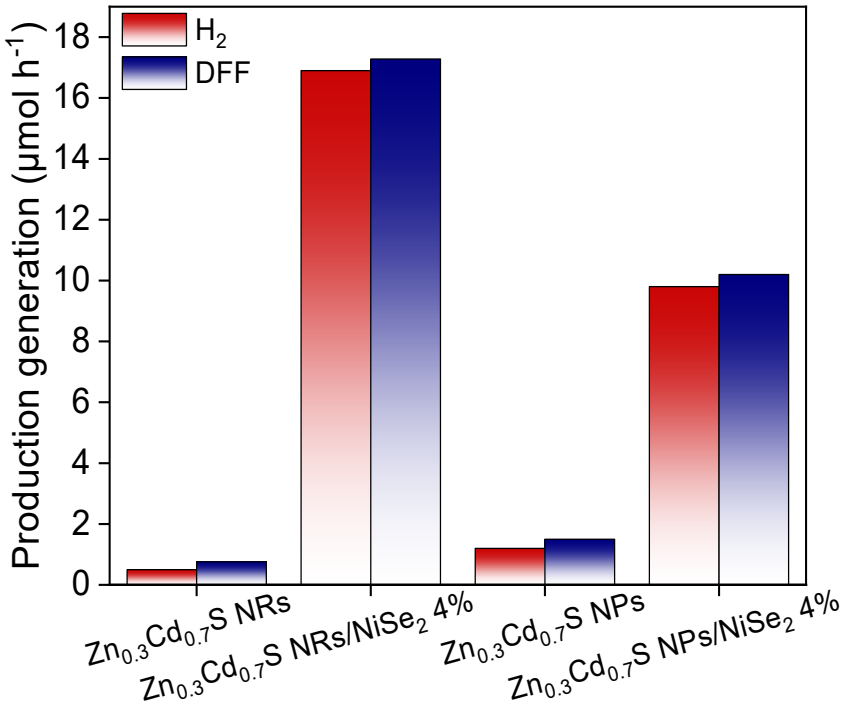

Figure S32. The photoactivity tests of selective HMF oxidation into DFF integrated with H_2 evolution over different $Cd_{0.7}Zn_{0.3}S$ and $Cd_{0.7}Zn_{0.3}S/NiSe_2$ composites.

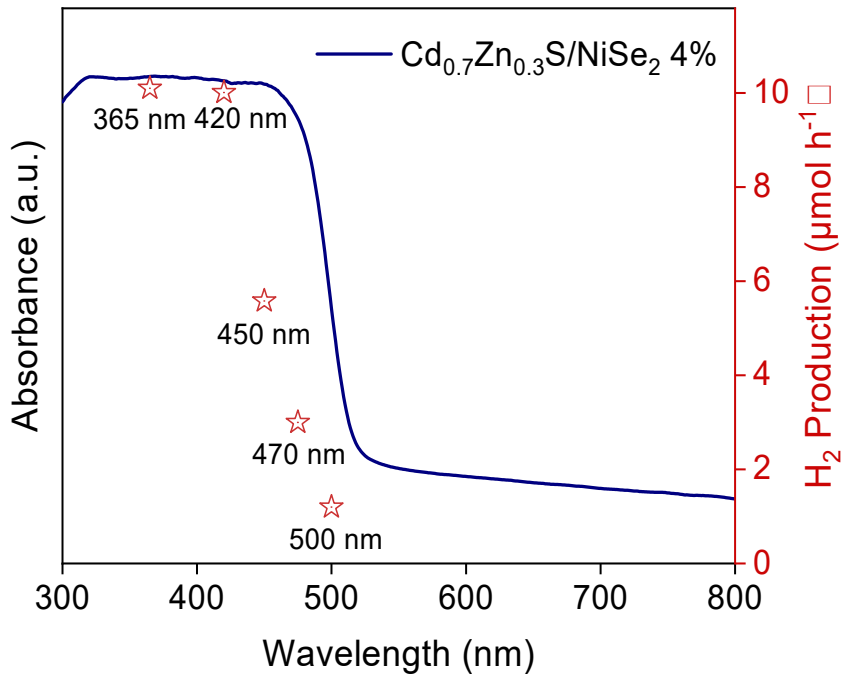

Figure S33. The photoactivity tests of selective HMF oxidation into DFF integrated with H_2 evolution under different wavelengths of light.

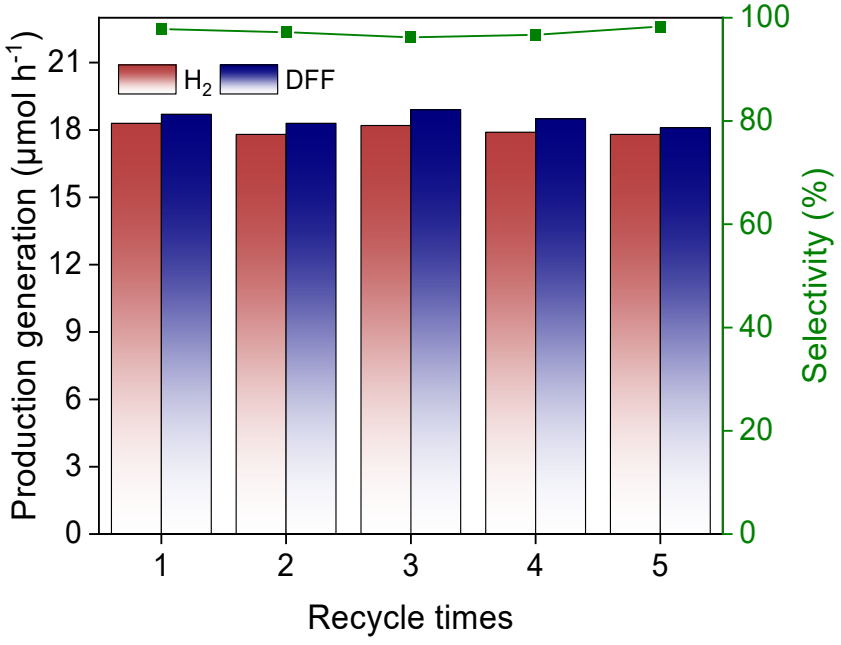

Figure S34. Photocatalytic cycle test of selective HMF oxidation into DFF integrated with H_2 over $Zn_{0.7}Cd_{0.3}S/NiSe_2$ 4%.

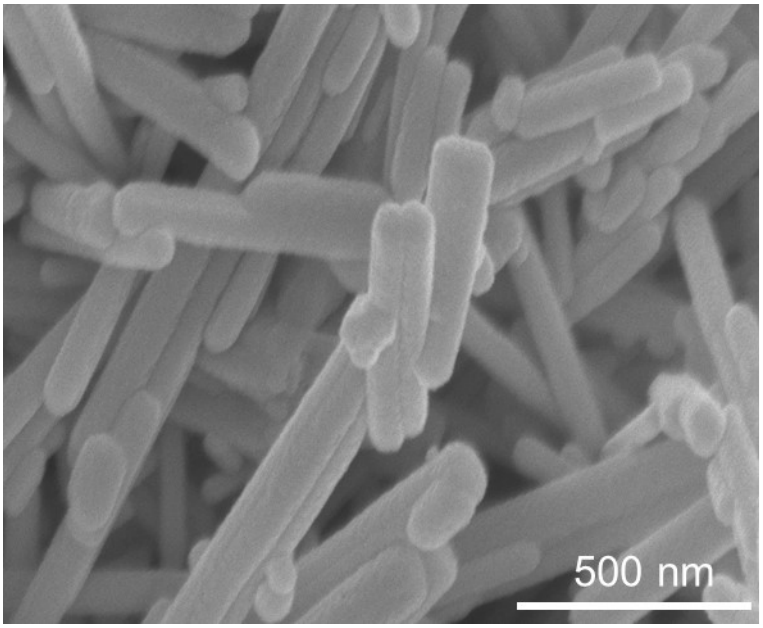

Figure S35. SEM image of $Cd_{0.7}Zn_{0.3}S/NiSe_2$ 4% after 11 h reaction.

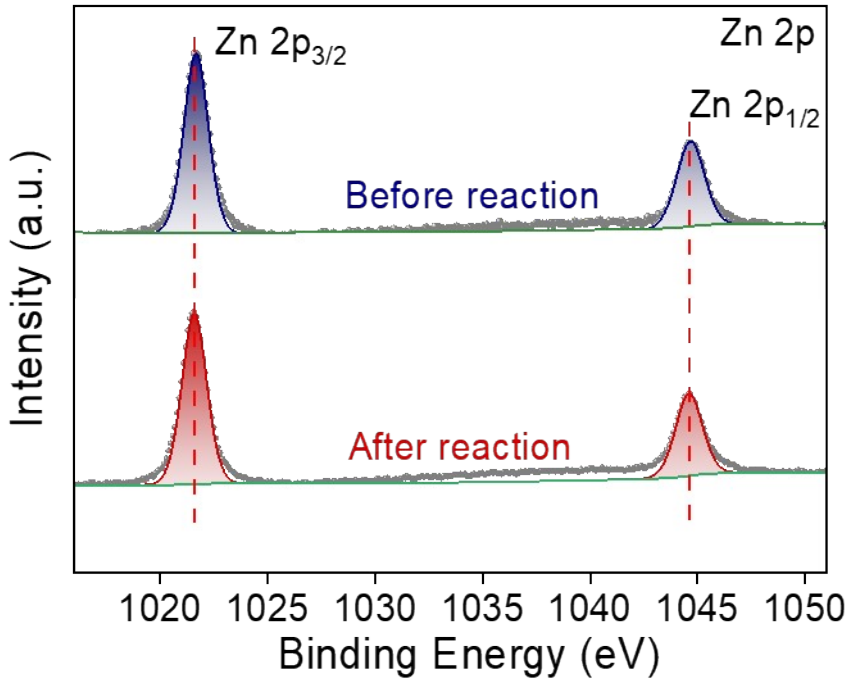

Figure S36. XPS spectra of Zn 2p of $Cd_{0.7}Zn_{0.3}S/NiSe_2$ 4% sample before reaction and after reaction.

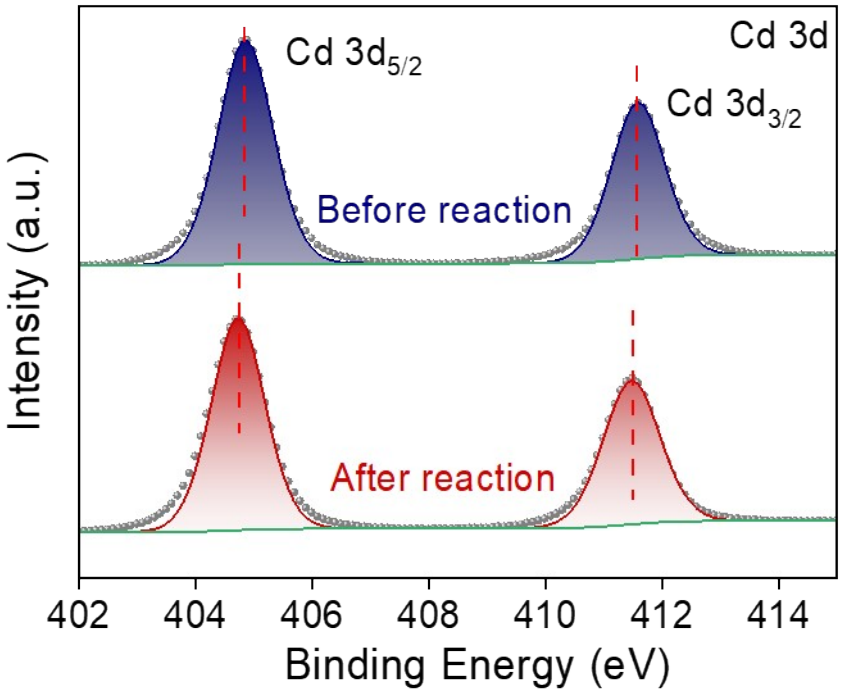

Figure S37. XPS spectra of Cd 3d of $Cd_{0.7}Zn_{0.3}S/NiSe_2$ 4% sample before reaction and after reaction.

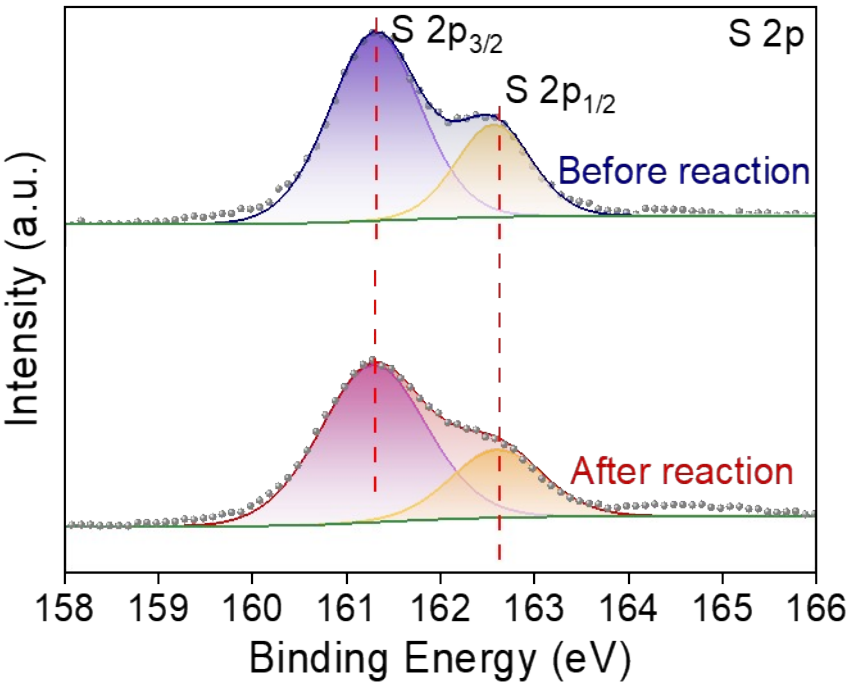

Figure S38. XPS spectra of S 2p of $Cd_{0.7}Zn_{0.3}S/NiSe_2$ 4% sample before reaction and after reaction.

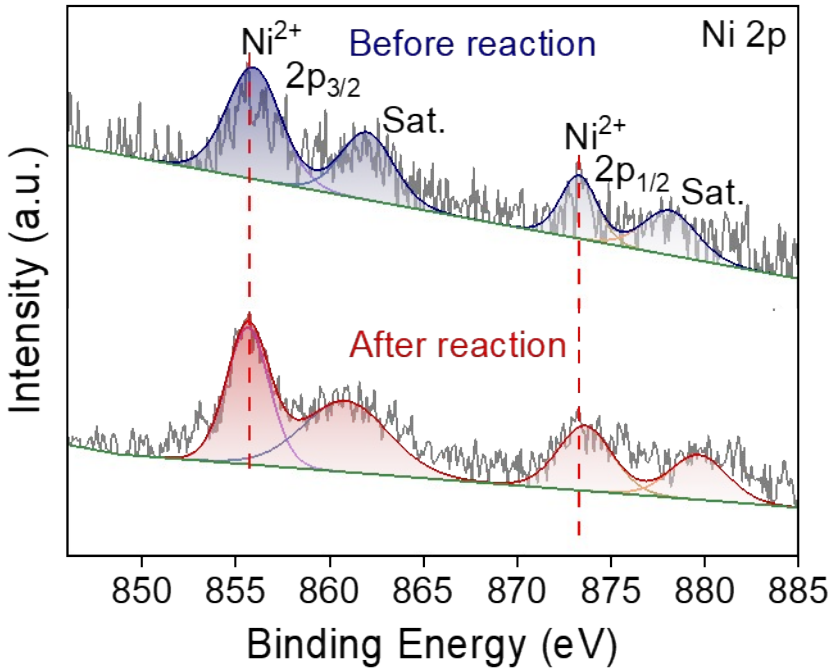

Figure S39. XPS spectra of Ni 2p of $Cd_{0.7}Zn_{0.3}S/NiSe_2$ 4% sample before reaction and after reaction.

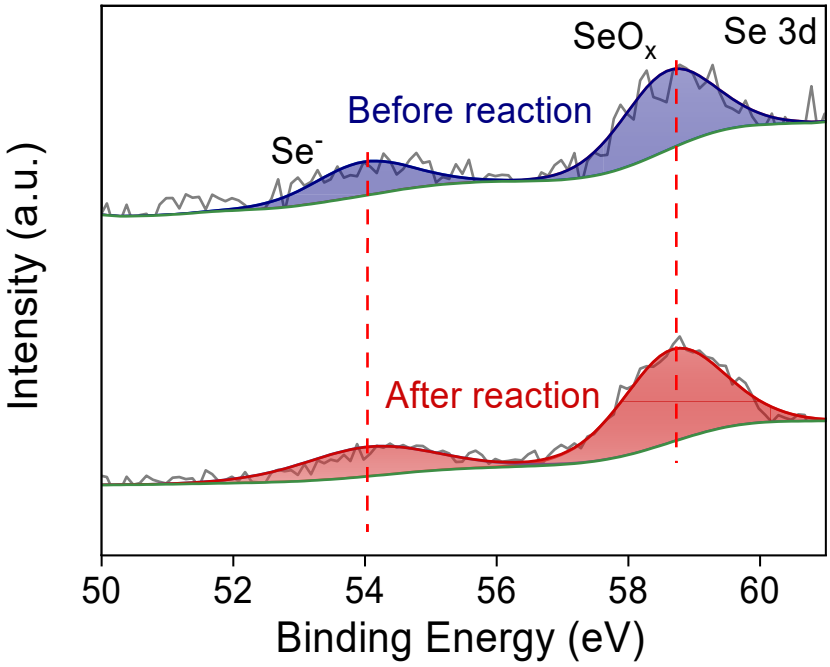

Figure S40. XPS spectra of Se 3d of $Cd_{0.7}Zn_{0.3}S/NiSe_2$ 4% sample before reaction and after the reaction.

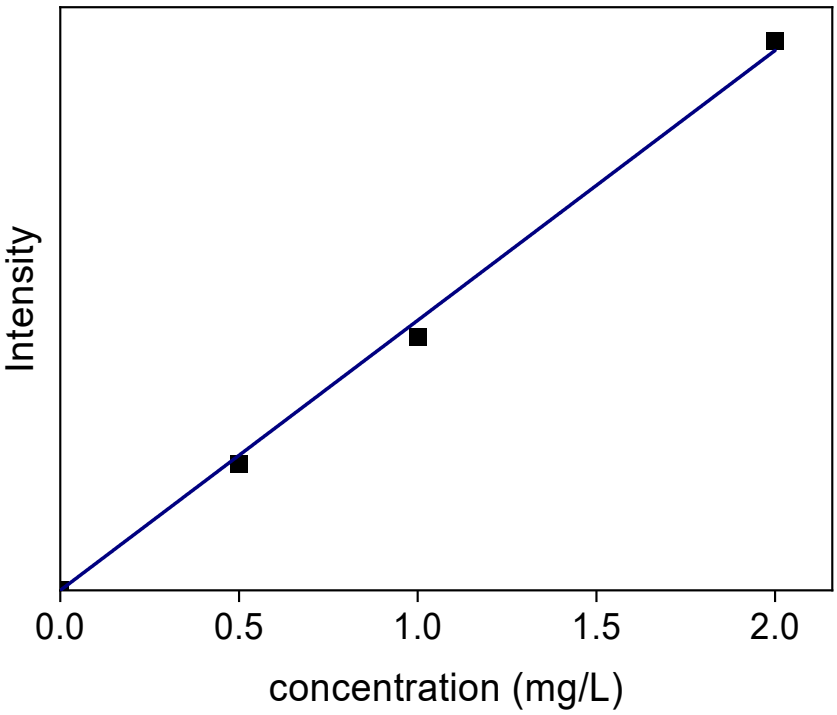

Figure S41. Standard curve of the ICP-OES for Cd^{2+}.

Table S1. Photocatalytic performance of selective oxidation of HMF to DFF in relevant research.

Entry	Catalyst	Light source	H_2 production rate (μmol g^{-1} h^{-1})	DFF production rate (μmol g^{-1} h^{-1})	Atmosphere	Reference
1	$Zn_{0.5}Cd_{0.5}S/MnO_2$	λ ≥ 400 nm, 30 × 3 W LED	55	46	N_2	[1]
2	UCNT/Pt	λ ≥ 400 nm, 300 W Xe lamp	92	95	vacuum	[2]
3	$Zn_{0.5}Cd_{0.5}S$-P	30 × 3 W LED	786	367	Ar	[3]
4	$NiS/Zn_3In_2S_6$	λ ≥ 420 nm, 300 W Xe lamp	120	129	N_2	[4]
5	$MAPbBr_3$	λ ≥ 450 nm，blue LED light	-	106	Air	[5]
6	CN-WO_3	λ ≥ 420 nm，10 W LED	-	36	Air	[6]
7	$MoS_2/CdIn_2S_4$	λ ≥ 420 nm， 7 W LED	-	50	Air	[7]
8	g-C_3N_4/Pd	300 W Xe lamp	-	250	N_2	[8]
9	Au-Ru/rGO	300 W Xe lamp	-	1328	O_2	[9]
10	CoP/ZCS	λ ≥ 420 nm, 300 W Xe	600	400	vacuum	[10]
11	$Cd_{0.7}Zn_{0.3}S/NiSe_2$	λ ≥ 400 nm, 300 W Xe	1690	1728	Ar	This work

Table S2. ICP-OES test of $Cd_{0.7}Zn_{0.3}S/NiSe_2$ x%.

10 mg $Cd_{0.7}Zn_{0.3}S/NiSe_2$ x%	5%	8%	10%	11%
Theoretical mass	0.5 mg	0.8 mg	1 mg	1.1 mg
Actual mass	0.25 mg	0.35 mg	0.40 mg	0.46 mg

Table S3. Structural parameters of photocatalysts obtained from N_2 adsorption-desorption analysis.

Catalyst	Specific surface area (m^2/g)	Mean pore diameter (nm)	Pore volume (cm^3/g)
$Cd_{0.7}Zn_{0.3}S$	22.4	34.7	0.19
$Cd_{0.7}Zn_{0.3}S/NiSe_2$ 4%	19.3	34.9	0.17

References

1. S. Dhingra, T. Chhabra, V. Krishnan and C. M. Nagaraja, *ACS Appl. Energy Mater.*, 2020, **3**, 7138-7148.
2. X. Bao, M. Liu, Z. Wang, D. Dai, P. Wang, H. Cheng, Y. Liu, Z. Zheng, Y. Dai and B. Huang, *ACS Catal.*, 2022, **12**, 1919-1929.
3. H.-F. Ye, R. Shi, X. Yang, W.-F. Fu and Y. Chen, *Appl. Catal., B*, 2018, **233**, 70-79.
4. S. Meng, H. Wu, Y. Cui, X. Zheng, H. Wang, S. Chen, Y. Wang and X. Fu, *Appl. Catal., B*, 2020, **266**.
5. M. Zhang, Z. Li, X. Xin, J. Zhang, Y. Feng and H. Lv, *ACS Catal.*, 2020, **10**, 14793-14800.
6. H. Qian, Q. Hou, W. Zhang, Y. Nie, R. Lai, H. Ren, G. Yu, X. Bai, H. Wang and M. Ju, *Appl. Catal., B*, 2022, **319**.
7. Q. Zhu, Y. Zhuang, H. Zhao, P. Zhan, C. Ren, C. Su, W. Ren, J. Zhang, D. Cai and P. Qin, *Chin. J. Chem. Eng.*, 2022, DOI: 10.1016/j.cjche.2022.04.018.
8. A. E. ElMetwally, M. S. Sayed, Y. Zhou, J. B. Domena, J.-J. Shim, R. M. Leblanc, M. R. Knecht and L. G. Bachas, *J. Phys. Chem. Lett.*, 2022, **126**, 15671-15684.
9. B. Ma, Y. Wang, X. Guo, X. Tong, C. Liu, Y. Wang and X. Guo, *Appl. Catal., A*, 2018, **552**, 70-76.
10. Y. Yang, W. Ren, X. Zheng, S. Meng, C. Cai, X. Fu and S. Chen, *ACS Appl. Mater. Interfaces*, 2022, **14**, 54649-54661.